The following publication Z. Situ, I. W. -H. Ho, Y. Hou and P. Li, "The Feasibility of NOMA in C-V2X," IEEE INFOCOM 2020 - IEEE Conference on Computer Communications Workshops (INFOCOM WKSHPS), Toronto, ON, Canada, 2020, pp. 562-567 is available at https://dx.doi.org/10.1109/INFOCOMWKSHPS50562.2020.9163009.

The Feasibility of NOMA in C-V2X

Zhenhui Situ*, Ivan Wang-Hei Ho*†, Yun Hou‡, and Peiya Li§
*Department of Electronic and Information Engineering, The Hong Kong Polytechnic University, Hong Kong
†Research Institute for Sustainable Urban Development, The Hong Kong Polytechnic University, Hong Kong
‡Technological and Higher Education Institute of Hong Kong, Hong Kong
§College of Cyber Security, Jinan University, China
Email: z.situ@connect.polyu.hk, ivanwh.ho@polyu.edu.hk, aileenhou@vtc.edu.hk, lpy0303@jnu.edu.cn

***Abstract*—Cellular Vehicle-to-everything (V2X) becomes one of the most significant techniques in the 5G standard. It uses the PC5 sidelink interface to enable direct communications between the vehicle and everything, e.g., neighboring vehicles, the infrastructure, and pedestrians. To facilitate ultra-reliable low-latency communication (URLLC) in high dense vehicular networks, this paper studies the feasibility of non-orthogonal multiple access (NOMA) in C-V2X to improve the spectral efficiency. According to the orthogonal multiple access (OMA) based PHY layer as specified in the PC5 sidelink interface, we propose two NOMA receivers based on two techniques: successive interference cancellation (SIC) and joint decoding (JD). It is demonstrated that the two receivers can be easily implemented on current C-V2X communications with minor modifications. Simulation results show that the two NOMA approaches can reduce the block error rate (BLER) by up to 93.6% as compared with the conventional OMA approach. In general, JD receiver provides better BLER performance at the cost of higher computational complexity as compared to the SIC receiver.**

I. Introduction

Vehicular networks have been developed rapidly in the past decade. To adapt the high-speed mobility and short contact time in vehicular networks, direct wireless communications, e.g., vehicle-to-vehicle (V2V), vehicle-to-infrastructure (V2I), and vehicle-to-pedestrian (V2P), are enabled to achieve ultra-reliable low-latency communications (URLLC). Recently, the cellular-V2X (C-V2X) technology was proposed in the third generation partnership project (3GPP) release 14 [1]. There are two radio interfaces supported by the C-V2X standard: the cellular interface and the PC5 interface [2]. The first one supports V2I communications and the second one, which is based on direct sidelink, supports V2V communications. In addition to the safety use cases considered in the dedicated short-range communications (DSRC), the new standard aims to include more use cases such as advanced vehicle platooning, extended sensors, advanced driving, and remote driving [3]. Each terminal requires an increasing amount of resource channels for these applications. Besides, the increasing number of V2X-enabled vehicles on the road is going to congest the vehicular networks.

A promising technology to improve the spectrum efficiency and handle the massive vehicular communications is non-orthogonal multiple access (NOMA). By allowing terminals to access the channel non-orthogonally, NOMA is a potential solution for C-V2X communications to reduce the waiting time before transmissions in dense vehicular networks. The pioneer work [4] exploited NOMA to alleviate the performance degradation in terms of latency and packet reception probability caused by the high density of vehicles. The proposed scheme includes centralized sub-channel allocation and distributed transmission power adjustment, and the work depends on eNodeB to perform centralized resource allocations. C-V2X communications can operate without the coverage of eNodeBs and the vehicles independently select radio resources. It has been verified by several recent works that NOMA can be employed for such uncoordinated transmissions [5]–[7]. Based on multi-channel ALOHA [8], Choi [5] proposed a NOMA system with a channel-dependent selection for sub-channel and power level, the system provided higher goodput than the orthogonal multiple access (OMA) based ALOHA. Seo et al. [6] studied NOMA random access (NORA) with multiple levels of target power based on channel inversion. This assures that the received power at the BS can be one of the two target values to guarantee the power difference for SIC, and the maximum goodput can be improved from 0.368 to 0.7 as compared with OMA. Decentralized broadcasting-NOMA (DB-NOMA) was proposed in [7] and an enhanced decentralized mode for C-V2X was designed to increase the node accommodation capacity (NAC) in Crash Warning System (CWS). The NAC can be improved by 119% when compared with the current standard.

However, the practical design of C-V2X physical layer is still not clear. Currently, there are two well-known multi-user detection (MUD) techniques for extracting overlapping signals: successive interference cancellation (SIC) and joint decoding (JD) [9]. The first one harnesses the power differences among multiple users and decodes them in sequence according to their received signal strengths. When the strongest user is decoded by regarding signals from other users as interference, the corresponding signal is canceled and the next user can be decoded without the interference from stronger users. For JD, the superimposed signals are jointly decoded, i.e., the combinations of transmitted symbol vectors from all users are exhausted. Under the operation of the centralized resource allocation, it is easy to exploit the power difference for SIC-based receivers when the radio channels are stable. However, the radio channels in vehicular networks change rapidly [10] and centralized resource allocation is infeasible in area without the coverage of eNodeBs. Therefore, it is difficult

to guarantee the power difference in C-V2X communications and JD is a potential solution. This paper aims to investigate the integration of NOMA and C-V2X communications, while the PC5 sidelink interface enabled for direct communications so that packets do not pass through eNodeBs. Based on the C-V2X physical layer as specified in the 3GPP Release 14, three receivers based on various receiving techniques, i.e., the conventional OMA receiver, SIC-based NOMA receiver, and JD-based NOMA receiver, are studied in this paper. We demonstrate that NOMA can be easily implemented on current C-V2X communications with minor modifications on the receiver.

II. Physical layer of C-V2X

In C-V2X communications, the time-frequency resource pool is divided into resource blocks (RBs) as shown in Fig. 1 and the transmitted data are modulated with single-carrier frequency-division multiple access (SC-FDMA).

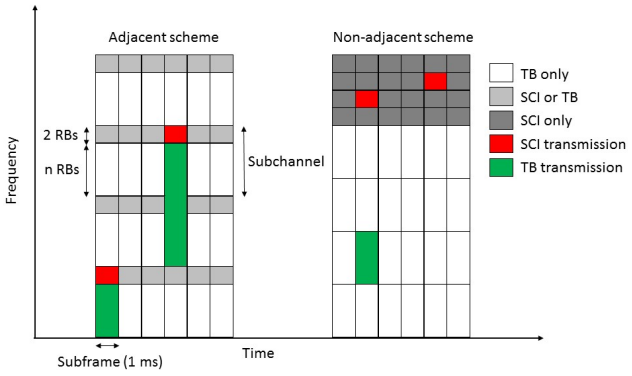

Fig. 1. C-V2X resource blocks.

According to the standard, C-V2X supports both 10 and 20 MHz channel width. For each channel, it is divided into sub-frames, sub-channels, and RBs. The smallest resource that can be assigned to a user is a RB. It consists of 12 sub-carriers with 15 kHz bandwidth, thus, the entire bandwidth of a RB is 180 kHz. In C-V2X, sub-channels are defined as a group of RBs in the same sub-frame. Depending on the communication requirement, one sub-channel can be assigned with different number of RBs. Sub-channels are utilized to transmit control information and data. There are two types of channels in C-V2X:

1) Physical sidelink shared channel (PSSCH): It transmits transport blocks (TBs) that contain a full packet, such as the basic safety message (BSM) and multimedia content for infotainment services. Since the packet size to be transmitted for each user varies, one user can occupy multiple TBs. Thus, the channel resource cannot be assigned orthogonally in a congested vehicular network, especially when some users are transmitting large packets for video streaming. To solve the problem, we utilize NOMA for TBs transmission over PSSCH, and NOMA-based receivers are employed to decode the overlapping messages from multiple users.
2) Physical sidelink control channel (PSCCH): It is used to transmit sidelink control information (SCI) messages. Basically, the information contained in SCI is used for TB transmission, and all TBs are associated with the corresponding SCIs. This is also known as the scheduling assignment. For instance, the SCI contains the PSCCH resource allocation for the TB, the modulation and coding scheme (MSC) used to transmit the TB, and the resource reservation interval for semi-persistent scheduling (SPS). The SCI messages include the necessary information to decode the data in TBs, thus the failure of SCI decoding means that the corresponding TB transmission fails. Each SCI message occupies two RBs, the size of SCI is relatively small compared with that of TBs. Since SCI contains the critical information for TB transmission and it only needs a small amount of channel resources, we use OMA for SCI transmission over PSCCH.

For PSCCH and PSSCH, C-V2X provides two sub-channelization schemes as illustrated in Fig. 1: adjacent and non-adjacent schemes. In the adjacent scheme, the SCI and TB are transmitted in adjacent RBs. One SCI transmission requires two RBs while one TB transmission can occupy multiple sub-channels. For the second scheme, the RBs are divided into two dedicated pools for SCI and TB transmissions, respectively. In the proposed NOMA-based C-V2X communication schemes, the non-adjacent scheme is employed, and OMA-based SCI and NOMA-based TB transmissions are considered.

In each sub-frame, there are 14 symbols and four of them are dedicated to demodulation reference signals (DMRSs). Specifically, the third, sixth, ninth, and 12th symbols are selected as pilot symbols, the receivers use the DMRSs to estimate the radio channels and combat negative effect caused by the time-frequency-selective channels. In terms of modulation, SCIs are always modulated with QPSK while TBs can be modulated with either QPSK or 16-QAM. Besides, the normal cyclic prefix is employed against inter-symbol-interference (ISI) and turbo coding is used to improve the block error rate (BLER) performance.

III. Receiver design

After introducing the physical layer of C-V2X, this section presents the NOMA-based receiver design. Because the SCI is transmitted orthogonally over PSCCH, this paper assumes perfect SCI transmission and focuses on the non-orthogonal TB transmissions. Firstly, the conventional OMA receiver is introduced, followed by the SIC and JD receivers.

A. OMA receiver for C-V2X communications

Fig. 2 shows the block diagram of the conventional OMA receiver. After receiving the signals, the first step is to perform synchronization, the synchronized signals are then passed to the SC-FDMA demodulation block. After that, the DMRSs are

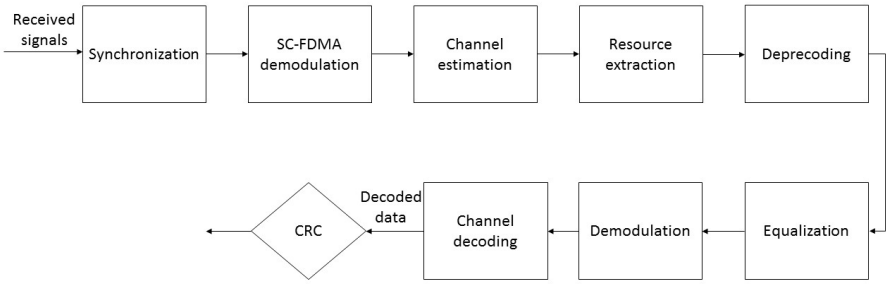

Fig. 2. Block diagram of the OMA receiver.

extracted to perform channel estimation. We assume perfect channel estimation in this paper and compare the performance of OMA, SIC-based NOMA, and JD-based NOMA receivers. After channel estimation, the data on the desired TB is extracted. The resource allocation information is obtained from the corresponding SCI messages. The next step is to perform deprecoding, namely the IFFT operation. Then, equalization is conducted to reverse the distortion incurred by the radio channel. Specifically, a minimum mean square error (MMSE) equalizer is employed in this work. Let X be the transmitted symbol, H is the channel, N is the complex white Gaussian noise with zero mean and variance N_o, the desired signal Y is

$$Y = HX + N. \tag{1}$$

Given M receiving antennas, H, N, and Y are $M \times 1$ matrices. After the MMSE equalization, the output signal $\hat{X}$ is as follows.

$$\hat{X} = (H^H H + N_o I)^{-1} H^H Y. \tag{2}$$

Where I is the identity matrix, and we utilize $[.]^{-1}$ and $[.]^H$ to denote the inverse and hermitian transpose, respectively. Let $W = (H^H H + N_o I)^{-1} H^H$ and the variance of noise after MMSE equalization as $\hat{N}_o = W W^H N_o$. The output signal is then demodulated to obtain the log-likelihood ratio (LLR).

$$LLR(X(i)) = \log [\frac{p(X(i) = 0|Y)}{p(X(i) = 1|Y)}]. \tag{3}$$

With

$$p(X(i) = j|Y) \propto \sum_{X(i)=j} \exp{(-\frac{|X - \hat{X}|^2}{\hat{N}_o})}. \tag{4}$$

Where $X(i)$ denotes the i-th bit of the transmitted symbol. To reduce the computational complexity, we employ a simple log-max approximation as follows.

$$p(X(i) = j|Y) \propto \max_{X(i)=j} \exp{(-\frac{|X - \hat{X}|^2}{\hat{N}_o})}. \tag{5}$$

The demodulated soft LLR is used for channel decoding and the result is passed to perform cyclic redundancy check (CRC).

For non-orthogonal C-V2X communications, the receivers need to decode multiple users from the superimposed signals. We propose two NOMA receivers based on SIC and JD.

B. SIC-based NOMA receiver for C-V2X communications

The block diagram of the SIC-based NOMA receiver is illustrated in Fig. 3. For the SIC-based NOMA receiver, the block diagram is basically the same as that of the OMA receiver. For instance, equalization is performed for the strongest user while the interference from other users is regarded as noise. Assuming that the overlapping signals from K transmitters and the user index k determines the decoding order, namely the received power level P_k from user k follows $P_i \geq P_k, \forall i \leq k$, without loss of generality. For user k, the MMSE equalization is performed as

$$\hat{X_k} = [H_k^H H_k + (\hat{N}_o + \sum_{i=k+1}^{K} P_i) I]^{-1} H_k^H Y, \tag{6}$$

where H_k is the channel state information (CSI) for user k. The summation of power from users $k+1$ to K is regarded as part of the noise. The channel decoding result is passed to the CRC check. Once the desired packet of user k is decoded correctly, it is used to perform interference cancellation and thus, the decoding of the remaining users can be performed in the absence of interference from user k.

C. JD-based NOMA receiver for C-V2X communications

For the JD-based NOMA receiver, the block diagram is shown in Fig. 4. For the synchronization, the frame offset of the strongest user is evaluated and we perform the corresponding synchronization for all users. In this work, we consider that K users occupy the same RBs for TB transmissions, thus we can conduct the same SC-FDMA demodulation, resource extraction, and deprecoding for all users. Besides, individual channel decoding is adopted to reduce the computational complexity. Even though joint channel decoders are expected to provide a better performance, this work focuses on the equalization and demodulation parts, and the joint channel decoder design is a potential future research direction. Since it is possible that only a portion of users is successfully decoded after the first iteration, the JD-based NOMA receiver includes interference cancellation to eliminate the signals from the decoded users to reduce the computational complexity of the

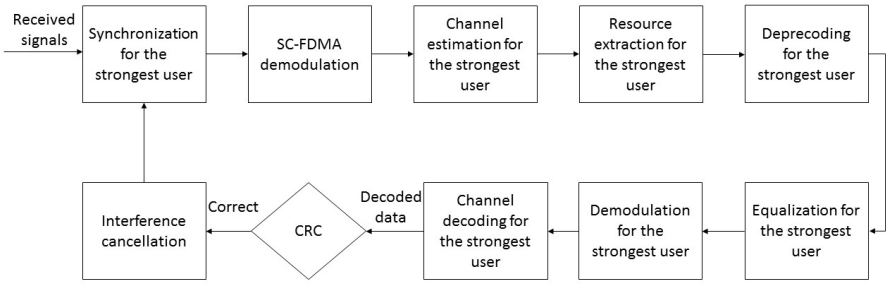

Fig. 3. Block diagram of the SIC-based NOMA receiver.

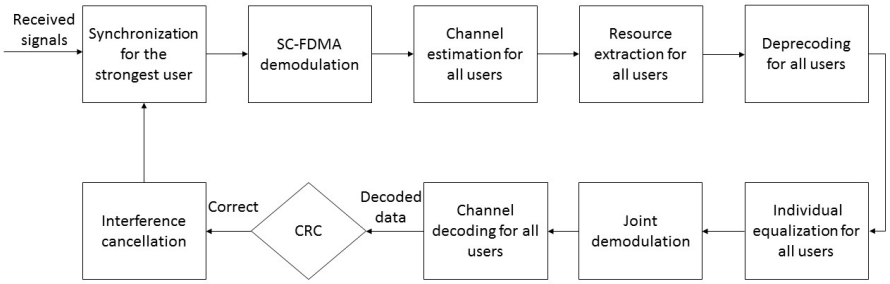

Fig. 4. Block diagram of the JD-based NOMA receiver.

following iterations. When no user can be decoded after an iteration, the receiver is interrupted.

Since the LLRs of individual users are required to perform the conventional channel decoding, this work proposes an individual equalization scheme for all users and performs joint demodulation to obtain the LLRs of individual users by taking the transmitted signals from remaining users into consideration.

In terms of individual equalization, the proposed scheme makes uses of the CSI from all users and aims to minimize the mean square error. For the first iteration, we aim to minimize the mean square error of user k as follows.

$$\min_{W_k} \mathbb{E}\{(W_k Y - X_k)(W_k Y - X_k)^H\}. \tag{7}$$

Let $G_k = [H_1, H_2, ..., H_{k-1}, H_{k+1}, ..., H_K]$ denotes the CSI of the remaining users. By solving the optimization problem in (7), the optimal matrix W_k can be obtained as follows.

$$W_k = [I + H_k^H (N_o + G_k G_k^H)^{-1} H_K]^{-1} H_k^H (N_o I + G_k G_k^H)^{-1}. \tag{8}$$

It can be observed that compared with the SIC-based equalizer in (6) where the average power P_i over the whole sub-channel from user i is regarded as part of the noise, the proposed JD-based equalizer takes the exact CSI of all the remaining users into consideration to minimize the mean square error. Since the optimal transformation matrices for all users can vary, the transformation matrices W_k for all users and the signals Y are sent from the equalizer to the joint demodulator. The proposed joint demodulator obtains the APP for user k as

$$p(X_k(i) = j|Y) \propto \max_{X_k(i)=j, X_1, X_2, ... X_{k-1}, X_{k+1}, ..., X_K} \exp\left(-\frac{|W_k Y - (\sum_{z=1}^{K} W_k H_z X_z)|^2}{N_o}\right). \tag{9}$$

Similar to (5), the joint demodulator obtains the LLR for user k as follows.

$$LLR(X_k(i)) = \log\left[\frac{p(X_k(i) = 0|Y)}{p(X_k(i) = 1|Y)}\right]. \tag{10}$$

IV. Simulation results

After introducing the C-V2X physical layer and the receiver design, we have shown that NOMA can be easily implemented on the current C-V2X communications with minor modifications on the receiver. This section aims to evaluate NOMA-based C-V2X communications. The simulation configuration is first introduced, it is then followed by the simulation results and the evaluation of the three schemes.

A. Simulation configuration

Following the C-V2X standard, we employ 10 MHz bandwidth and the total number of RBs is 50. QPSK modulation is adopted for TB transmission. The transmitters are assumed to be equipped with a single transmit antenna and the receivers are assumed to be equipped with either single or two receiving antennas. In terms of the radio model, the MIMO multi-path fading model as specified in TS 36.101 [11] and TS 36.104 [12] is adopted. Specifically, the delay

profile follows the Extended Vehicular A model (EVA) in [11], [12]. The generalized method for exact Doppler spread (GMEDS) in [13] is utilized to model the Rayleigh fading, and the maximum Doppler frequency is 500 Hz. Since this work focuses on random access without power control, all transmitters transmit with the same transmission power and the SNR is defined as the ratio of transmit signal power from each user to the noise power. The transmitted signals from all transmitters undergo independent radio channels. For each user, the summation of the powers of the taps defined in the delay profile follows independent exponential distribution $\exp(1)$. When the number of receiving antenna is larger than one, we consider two types of correlations between the transmission antennas and the receiving antennas: low or no and high correlations as defined in [11].

B. Non-orthogonal C-V2X communications with a single receiving antenna

We first consider the single receiving antenna case, the SNR varies from 0 to 10 dB. The single-user case with OMA receiver is also simulated as a benchmark. In this case, the three receivers are expected to provide the same performance and the lowest average BLER can be obtained due to interference-free communications. Then, the number of transmitters is increased from two to four, the results are illustrated in Table I.

TABLE I
AVERAGE BLER RESULTS WITH A SINGLE RECEIVING ANTENNA.

SNR/dB		0	5	10
1-user	OMA	0.48	0.18	0.05
2-user	OMA	0.74	0.54	0.44
	SIC	0.69	0.37	0.18
	JD	0.60	0.23	0.06
3-user	OMA	0.85	0.74	0.68
	SIC	0.82	0.58	0.40
	JD	0.72	0.35	0.09
4-user	OMA	0.91	0.85	0.82
	SIC	0.90	0.77	0.63
	JD	0.83	0.52	0.22

It can be observed that the JD receiver provides the lowest BLER among the three receivers, followed by the SIC receiver. The gaps among the three receivers increase as the SNR increases. Besides, the gap between the JD receiver and the other receivers ascend when the number of user increases. For the 4-user case at 10 dB SNR, the BLER of the JD receiver is 0.22 while that of the other schemes are higher than 0.6. JD receiver is the best choice given a large number of transmitters. Comparing the single-user case with OMA receiver and 4-user case with JD receiver, the average BLER difference is 0.17 given a high SNR at 10 dB and 0.35 given an SNR of 0 dB. This indicates that although NOMA can improve the spectrum efficiency and provides low BLER in the high SNR regime, we should carefully control the number of access users in the low SNR regime to guarantee reasonable BLER performance for practical applications.

C. Non-orthogonal C-V2X communications with two receiving antennas

In addition to the single receiving antenna, the two receiving antenna case is simulated. We first consider a high correlation between the two inputs and the simulation results are shown in Table II.

TABLE II
AVERAGE BLER RESULTS WITH TWO RECEIVING ANTENNAS (HIGH CORRELATION).

SNR/dB		0	5	10
1-user	OMA	0.25	0.08	0.03
2-user	OMA	0.57	0.42	0.37
	SIC	0.45	0.20	0.09
	JD	0.35	0.11	0.04
3-user	OMA	0.74	0.66	0.63
	SIC	0.62	0.39	0.27
	JD	0.46	0.15	0.04
4-user	OMA	0.86	0.80	0.78
	SIC	0.79	0.60	0.48
	JD	0.59	0.23	0.05

By looking at the results in Tables I and II, the BLER performances of the three receivers are improved by adopting a larger number of receiving antennas. For the 4-user case with 10 dB SNR, the BLER difference between the OMA and JD receivers is 0.73. This indicates that the BLER is reduced by 93.6%. Generally, the JD receiver still gives the best performance, but the gap between JD and SIC receivers is slightly shortened when the number of access users is lower than four. For instance, the BLER difference of the two receivers in the 2-user case with 5 dB SNR is reduced by 0.05 as compared with the single antenna case. This is because the SIC receiver requires certain power difference among multiple users and multiple receiving antennas increases the probability that the criteria is met. Then, the correlation between the two inputs is configured as low or no, and the results are shown in Table III. We can observe that the performance gap between the SIC and JD receivers is further shortened given a lower correlation between the two inputs, within which the power difference criteria can be met easier. This reveals that the performance gap between the SIC and JD receivers can be reduced by employing a larger number of receiving antennas with low or no correlation. Given multiple input channels with low correlation, the SIC receiver can provide similar performance as the JD receiver while requiring relatively low computational complexity.

V. CONCLUSION

This paper presents the implementation of NOMA in C-V2X systems as specified in 3GPP Release 14. Based on the PC5 sidelink interface that supports direct communications without forwarding by the eNodeBs, we have proposed two

TABLE III
AVERAGE BLER RESULTS WITH TWO RECEIVING ANTENNAS (LOW CORRELATION).

SNR/dB		0	5	10
1-user	OMA	0.22	0.07	0.02
2-user	OMA	0.43	0.28	0.22
	SIC	0.31	0.10	0.04
	JD	0.27	0.08	0.03
3-user	OMA	0.58	0.46	0.41
	SIC	0.41	0.15	0.06
	JD	0.32	0.09	0.03
4-user	OMA	0.69	0.60	0.57
	SIC	0.51	0.24	0.13
	JD	0.38	0.11	0.03

NOMA receivers for C-V2X communications: the SIC-based receiver and JD-based receiver. The two schemes are based on the conventional OMA-based C-V2X receiver with minor modifications. Several interesting points are obtained from the simulation results: i) the two NOMA schemes offer significant improvement as compared with the conventional OMA scheme, and the BLER can be reduced by up to 93.6%; ii) the JD receiver provides the best performance among the three receivers, and the BLER gaps are enlarged as the number of users increases; and iii) the performance gap between the SIC and JD receivers can be reduced by adopting a larger number of receiving antennas, especially when the correlation among multiple inputs is low.

ACKNOWLEDGMENT

This work was supported in part by the General Research Fund (Project No. 15201118) established under the University Grant Committee (UGC) of the Hong Kong Special Administrative Region (HKSAR), China; and by The Hong Kong Polytechnic University (Projects G-YBR2, G-YBXJ).

REFERENCES

[1] 3rd Generation Partnership Project, "Release 14," *URL http://www.3gpp.org/release-14*, 2016.

[2] R. Molina-Masegosa and J. Gozalvez, "LTE-V for sidelink 5G V2X vehicular communications: a new 5G technology for short-range vehicle-to-everything communications," *IEEE Vehicular Technology Magazine*, vol. 12, no. 4, pp. 30–39, 2017.

[3] 3GPP TS 22.186 (v.15.2.0), "Service requirements for enhanced V2X scenarios," *3rd Generation Partnership Project; Technical Specification Group Radio Access Network*.

[4] B. Di, L. Song, Y. Li, and G. Y. Li, "Non-orthogonal multiple access for high-reliable and low-latency V2X communications in 5G systems," *IEEE Journal on Selected Areas in Communications*, vol. 35, no. 10, pp. 2383–2397, 2017.

[5] J. Choi, "NOMA-based random access with multichannel ALOHA," *IEEE Journal on Selected Areas in Communications*, vol. 35, no. 12, pp. 2736–2743, 2017.

[6] J. B. Seo, B. C. Jung, and H. Jin, "Non-Orthogonal Random Access for 5G Mobile Communication Systems," *IEEE Transactions on Vehicular Technology*, vol. 67, no. 8, pp. 7867–7871, 2018.

[7] T. Hirai and T. Murase, "Noma concept for pc5-based cellular-v2x mode 4 in crash warning system," in *2019 IEEE 90th Vehicular Technology Conference (VTC2019-Fall)*. IEEE, 2019, pp. 1–6.

[8] W. Yue, "The effect of capture on performance of multichannel slotted ALOHA systems," *IEEE Transactions on Communications*, vol. 39, no. 6, pp. 818–822, 1991.

[9] Y. Zhang, K. Peng, Z. Chen, and J. Song, "SIC vs. JD: Uplink NOMA techniques for M2M random access," *Communications (ICC), 2017 IEEE International Conference on*, pp. 1–6, 2017.

[10] Z. Zhao, X. Cheng, M. Wen, B. Jiao, and C.-X. Wang, "Channel estimation schemes for ieee 802.11 p standard," *IEEE intelligent transportation systems magazine*, vol. 5, no. 4, pp. 38–49, 2013.

[11] 3GPP TS 36.101, "Evolved Universal Terrestrial Radio Access (E-UTRA); User Equipment (UE) Radio Transmission and Reception," *3rd Generation Partnership Project; Technical Specification Group Radio Access Network*.

[12] 3GPP TS 36.104, "Evolved Universal Terrestrial Radio Access (E-UTRA); Base Station (BS) Radio Transmission and Receptionn," *3rd Generation Partnership Project; Technical Specification Group Radio Access Network*.

[13] M. Patzold, C.-X. Wang, and B. O. Hogstad, "Two new sum-of-sinusoids-based methods for the efficient generation of multiple uncorrelated Rayleigh fading waveforms," *IEEE Transactions on Wireless Communications*, vol. 8, no. 6, pp. 3122–3131, 2009.